Experimental Studies on the Effect of Inlet Liquid Subcooling on the Chilldown Characteristics of Stainless Steel Tubes

Jayachandran K. Narayanan* and Chirag R. Kharangate†
Case Western Reserve University, 10900 Euclid Avenue, Cleveland, OH 44106, USA

Jason W. Hartwig‡
NASA Glenn Research Center, Cleveland, OH 44135, USA

Jeffrey R. Mackey§
HX5, LLC, 3000 Aerospace Parkway, Brookpark, OH 44142, USA

Mohammad Kassemi¶
National Center for Space Exploration Research (NCSER), NASA Glenn Research Center and Case Western Reserve University, Cleveland, OH, 44135, USA

Understanding transfer line chilldown process under microgravity is important for the efficient transfer of cryogenic propellants in space fuel depots to facilitate future long duration space missions. The present work is part of the ongoing efforts to develop and test a two-phase flow chilldown test section to study the complete chilldown process under sustained microgravity conditions onboard the International Space Station. In this study, ground-based chilldown experiments are carried out on a 60 cm long SS-316 test section with PF-5060 as the working fluid. The complete chilldown curve was obtained including the film, transition and nucleate boiling regimes along with the temperature transition points. The effect of inlet liquid subcooling on the behavior of the chilldown curves are presented. Further, the chilldown and heat flux curves are analyzed to obtain re-wetting/Leidenfrost and onset of nucleate boiling temperature transition points as well as the critical heat flux values. The effect of inlet liquid subcooling on regime-specific heat flux and heat transfer coefficients are also examined.

Nomenclature

$nPFH$	=	normal perflourohexane
$FBCE$	=	Flow Boiling and Condensation Experiment
PID	=	proportional–integral–derivative
LFP	=	Leidenfrost point
ONB	=	Onset of Nucleate Boiling
CHF	=	Critical Heat Flux
OD	=	Outer diameter
$rewet$	=	rewetting
$conv$	=	convective
T	=	temperature [K]
m	=	mass flow rate [g/s]
q	=	convective heat flux [kW/m^2]
h	=	heat transfer coefficient [W/m^{2}K]
FB	=	film boiling

*Postdoctoral Scholar, Department of Mechanical and Aerospace Engineering, Glennan 209Y, 10900 Euclid Avenue, Cleveland, OH 44106, USA, and AIAA Young Professional

†Assistant Professor, Department of Mechanical and Aerospace Engineering, Glennan 459B, 10900 Euclid Avenue, Cleveland, OH 44106, USA.

‡Research Aerospace Engineer, Fluids and Cryogenics Branch, 21000 Brookpark Road, Cleveland, OH, 44135, and AIAA Associate Fellow.

§Research Engineer, Optics and Imaging Specialty, 21000 Brookpark Road, Cleveland, OH, 44135, USA.

¶Research Professor, Department of Mechanical and Aerospace Engineering, and AIAA Associate Fellow.

TB = transition boiling
NB = nucleate boiling
$SPLC$ = single phase liquid convection

I. Introduction

EFFICIENT cryogenic transfer line chilldown processes play a crucial role in the success of future NASA space missions. Specifically, for the planned in-space cryogenic fuel depots for long duration space missions, the transfer of cryogenic liquids through metallic tubes under microgravity is of great significance. The chilldown of transfer lines has never been conducted in a sustained, microgravity environment. For this purpose, research efforts are being undertaken to study the chilldown process of simulant fluids like normal perflourohexane (nPFH) or FC-72 in a closed loop chilldown test section which can be integrated with the Flow Boiling and Condensation Experiments (FBCE) module onboard the International Space Station (ISS) [1]. In this work, the ground based experimental results for the closed loop SS-316 chilldown test section employing PF-5060 as the working fluid are presented.

Chilldown experiments with cryogenic fluids such as LN_2 [2–4], LH_2 [5], LOX [6, 7], LCH_4 [7] and LAr [8] have been reported in the literature which typically operate in an open cycle where the generated vapor is vented out. Further, transfer line quenching process under microgravity has been studied by various researchers using cryogenic as well as simulant fluids. Darr et al. [9] and Hartwig et al. [10] performed LN_2 chilldown experiments under microgravity onboard NASA's C-9 aircraft and Zero-G Corporation's Boeing 727 aircraft and obtained the complete microgravity chilldown curve for high Reynolds number cases through bare SS-304 tube where the total chilldown time was in the range of 15-20s. Chilldown experiments were also conducted using the simulant fluids such as R113 [11–13] and FC-72 [14, 15] onboard parabolic flights which typically operates in a closed loop cycle to avoid venting out the generating vapor. The microgravity chilldown experiments reported above are limited by the microgravity environment duration onboard parabolic flights and the proposed FBCE-Transfer Line (FBCE-TL) experiments aim to conduct chilldown experiments onboard pure and sustained microgravity conditions onboard ISS.

As discussed earlier, the focus of the present research is to demonstrate a ground based experimental setup for chilldown experiments operating in a closed loop cycle for performing experiments onboard ISS for a wide range of operating conditions under pure and sustained microgravity conditions. The present chilldown experiments captured all the regimes of a typical chilldown process including the film, transition and nucleate boiling as well as the single phase liquid convective flow regimes. Further, in this paper, the focus is narrowed down to study the effect of inlet liquid subcooling on the chilldown characteristics as the liquid inlet temperature plays a major role in the rate of heat transfer and phase change in a typical chilldown process. The chilldown experiments are performed in a horizontal flow configuration SS-316 tube of $0.375''$ outer diameter, $0.065''$ thickness and 60 cm long with PF-5060 as the working fluid. Outer wall temperature measurements are presented to obtain the chilldown curves and the temperature transition points such as rewetting/Leidenfrost (LFP) temperature and onset of nucleate boiling (ONB) temperature. Inverse heat conduction laws are applied to estimate the heat flux curves and critical heat flux at different inlet subcooling conditions. Finally, the effect of inlet subcooling on the regime-specific time-averaged heat fluxes and heat transfer coefficients are presented at various wall locations.

II. Experimental Setup and Methodology

A. Details of the experimental chilldown test section

A typical flow conditioning loop for flow boiling experiments provide the working fluid at desired inlet conditions such as mass flow rate, temperature, quality and pressure to the flow boiling test section [1, 16]. The details of the flow conditioning loop for the present experiments is discussed in Narayanan et al. [17], which provides the working fluid PF-5060 at the desired inlet conditions to the chilldown test section. The chilldown test section for the present experiments is as shown in Fig. 1, which is comprised of a main loop and a bypass loop. The purpose of the bypass loop is to divert the working fluid during the pre-heating of the test section to the desired initial wall temperature, so that the fluid will attain steady conditions before entering the chilldown test section. The SS-316 chilldown test tube is heated by means of fibre-glass insulated Nichrome tape heater which is winded around the tube as uniform as possible. A check valve with a cracking pressure of around 1 psi is connected after the outlet of the main test section to allow excess liquid to flow back into the loop to accommodate the vapor generation in the preheating stage. The pre-heating stage is a temperature controlled process where the temperature of the outer wall is used as a feedback for the PID and

power controllers.

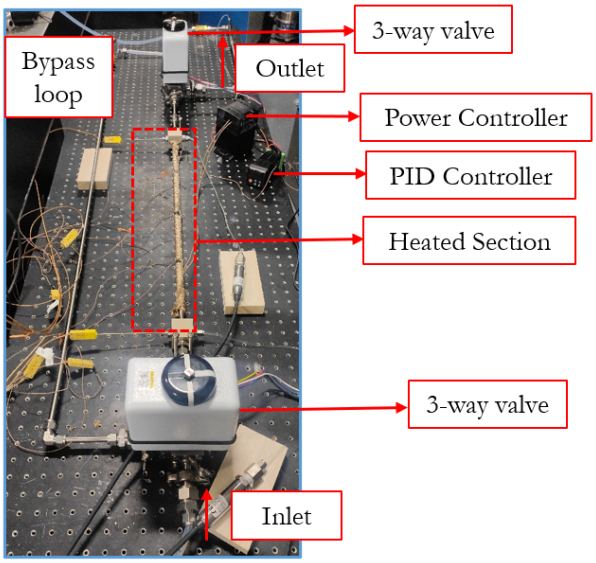

Fig. 1 Chilldown test section.

The 0.375″ OD, 0.065″ thickness SS-316 test section with the temperature and pressure measurements is depicted in Fig. 2 with PF-5060 as the working fluid. The test section is 60 cm long with outer wall temperature measurements at a distance of 15 cm apart on the top and bottom sides of the tube. The inlet and outlet fluid pressures and temperatures are measured by attaching the sensors in a specially designed PEEK block as shown in Fig. 2. Further, the tape heater is used to increase the outer wall temperature to around 250 ^{0}C before initiating the chilldown tests. During the pre-heating phase, it is observed that the generated bulk vapor is in saturated conditions with spikes in pressures during the onset of nucleate boiling stage [17]. The pressure spikes eventually dampens out as heating progresses and the chilldown tests are initiated once the wall thermocouples read above 250 ^{0}C by diverting the flow from the bypass loop to the main test section using a three-way valve shown in Fig. 1.

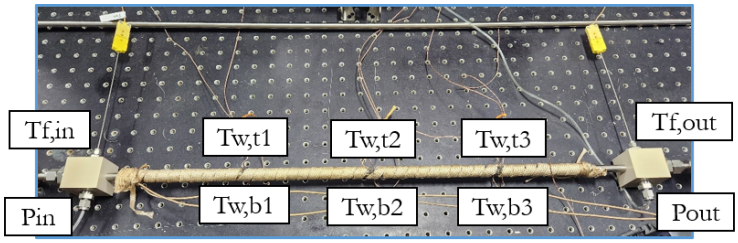

Fig. 2 Temperature and pressure measurements along the chilldown test section.

B. Experimental test cases

To elucidate the effect of inlet liquid subcooling on the chilldown process, experiments are performed at 7 different inlet temperature values as shown in Table 1. As the distance between the bulk fluid preheater and the test section inlet is high in the present setup, going below inlet subcooling of 7.3 ^{0}C generated two-phase flow after the bulk preheater. Hence, the bulk preheater and the test section inlet needs to be close enough to test saturated and two-phase inlet conditions in future. At low inlet subcoolings, the inlet mass flow rate also varies which may be attributed to the generation of vapor in some parts of the flow conditioning loop.

Table 1 Experimental test runs

Runs	Inlet mass flow rate (g/s)	Inlet pressure (kPa)	Inlet temperature (^{0}C)	Inlet subcooling (^{0}C)
1	7.15	109.35	51.9	7.3
2	7.32	113.14	49.3	10.9
3	7.48	111.56	43.1	16.7
4	7.40	109.90	36.4	22.9
5	7.46	105.83	32.5	25.7
6	7.49	105.01	28.6	29.4
7	7.45	103.63	23.4	34.2

III. Results and Discussion

A. Chilldown curves

To obtain the effect of inlet liquid subcooling on the chilldown process, as shown in Fig. 3, the chilldown curves for three different inlet subcoolings have been presented at different wall locations.

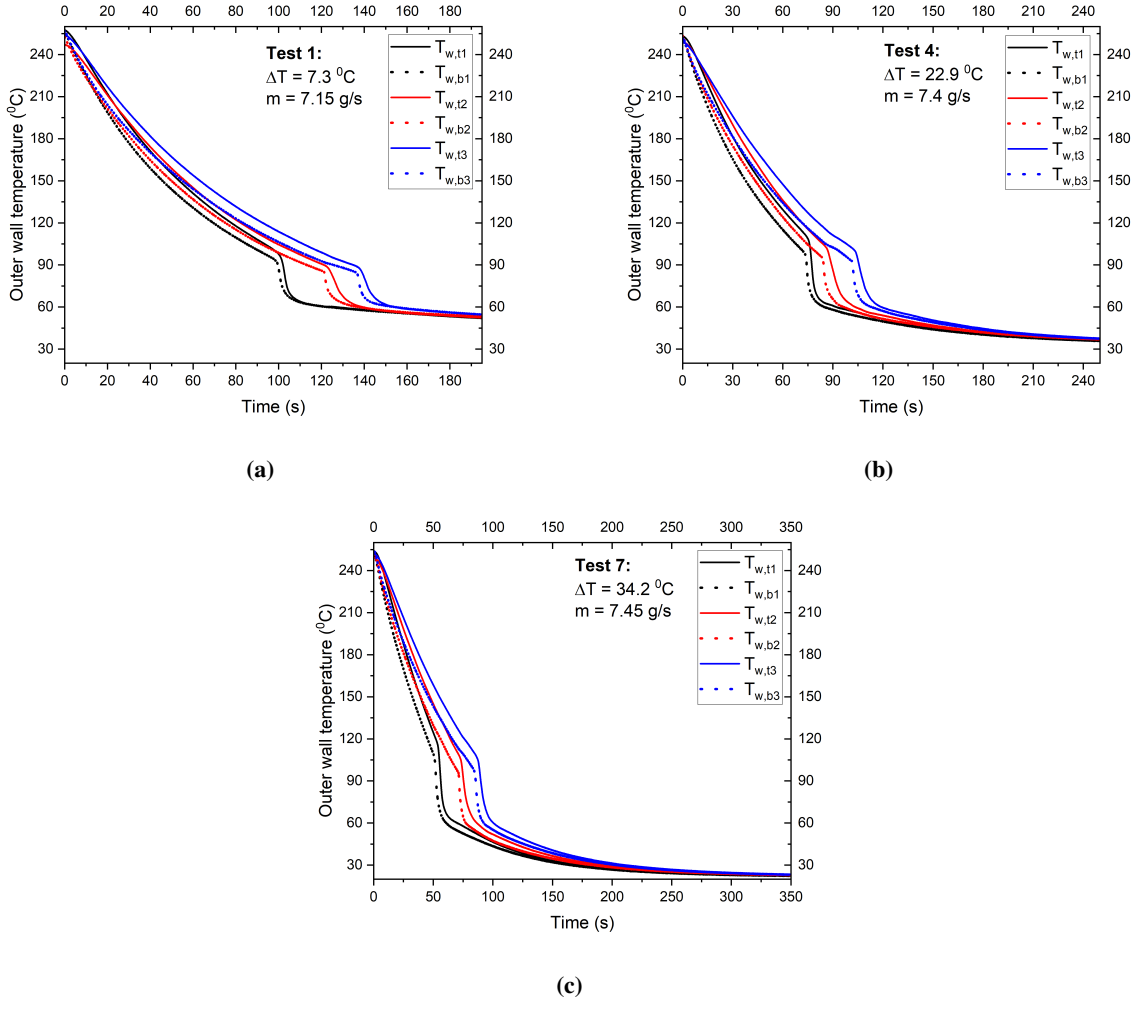

Fig. 3 Effect of inlet liquid subcooling on the chilldown curves at different outer wall locations

The chilldown curve is characterised by the film, transition and nucleate boiling regimes as well as the single phase liquid convective flow regimes. The present experiments captured all these regimes for PF-5060 and the behavior is similar to the reported cryogenic chilldown curves in the literature [2]. At low inlet liquid subcoolings, the chilldown curves indicate a longer duration film boiling regime which is common for cryogenic chilldown process where the inlet fluid is near saturation conditions. Also, it can be seen that the duration of single phase liquid convective regimes reduce as the inlet subcooling decreases. Due to the effect of gravity, the tube cools down faster at bottom walls compared to top walls for all the inlet subcooling tests. Along the axial direction from the inlet, the upstream locations cool down faster compared to the downstream locations as the quench front propagates through the tube.

B. Rewetting and ONB temperature points

To understand the effect of inlet liquid subcooling on the chilldown curve to some more detail, the temperature transition points, the rewetting and ONB temperatures are plotted in Figs. 4a and 4b respectively. The temperature transition points are characterised by the change in slope of the chilldown curve and is obtained by evaluating the second order derivative of the chilldown curve.

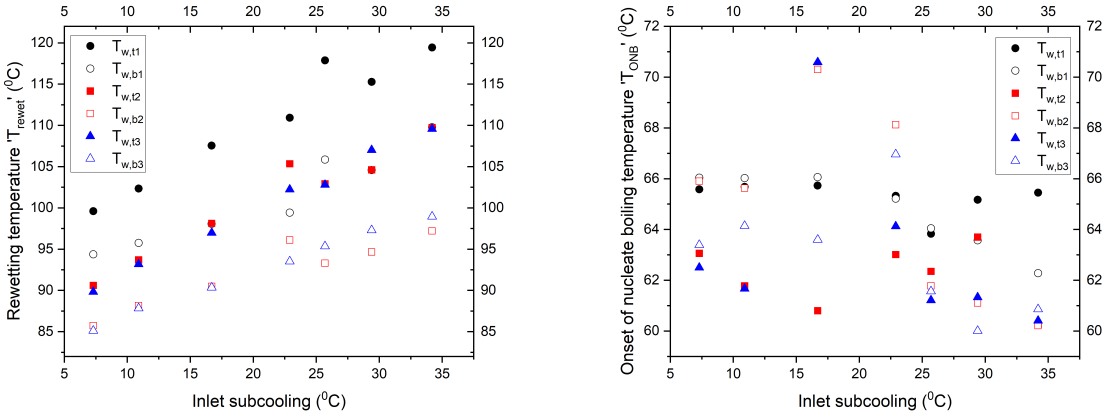

(a) **(b)**

Fig. 4 Effect of inlet liquid subcooling on the rewetting and ONB temperatures at different wall locations

From Fig. 4a, it can be observed that the rewetting temperatures increase with increase in inlet subcooling. Also, due to the effect of gravity, the top walls show a higher rewetting temperature compared to the bottom walls. The rewetting temperature at the upstream location 1 is higher than the downstream locations 2 & 3, which are close to each other for both top and bottom wall locations. In the case of ONB temperatures as shown in Fig. 4b, no definitive trends were observed due to the fluctuations in data.

C. Heat flux curves and critical heat flux

With the help of inverse heat conduction laws reported in Darr et al. [2] originally formulated by Burggraf [18], the heat flux curves are obtained from the outer wall temperature data. The parasitic heat losses are accounted by means of estimating the natural convection and radiation heat transfer from the outer surface of the tube to the surroundings. The heat flux curves at different inlet liquid subcoolings and wall locations are plotted as shown in Fig. 5.

The change in slope within the film boiling regime at the start of chilldown indicates the presence of dispersed droplets regime before the inverted annular film boiling regime kicks in. The heat flux values decrease as the thickness of the vapor film reduces in time until the rewetting point, at which the heat flux values start to increase in the transition boiling regime. At the end of the transition boiling regime, the heat flux reaches the maximum value representing the critical heat flux after which the values decrease in the nucleate boiling regime. At the ONB point, the slope of the heat flux curve changes again leading to the single phase liquid convective regime. In general, the bottom walls show a higher convective heat flux compared to the top walls due to the effect of gravity.

Further, the critical heat flux values at different inlet liquid subcooling and wall locations are plotted as shown in Fig. 6. The CHF values tend to increase with increase in inlet liquid subcooling and the bottom wall CHFs are either

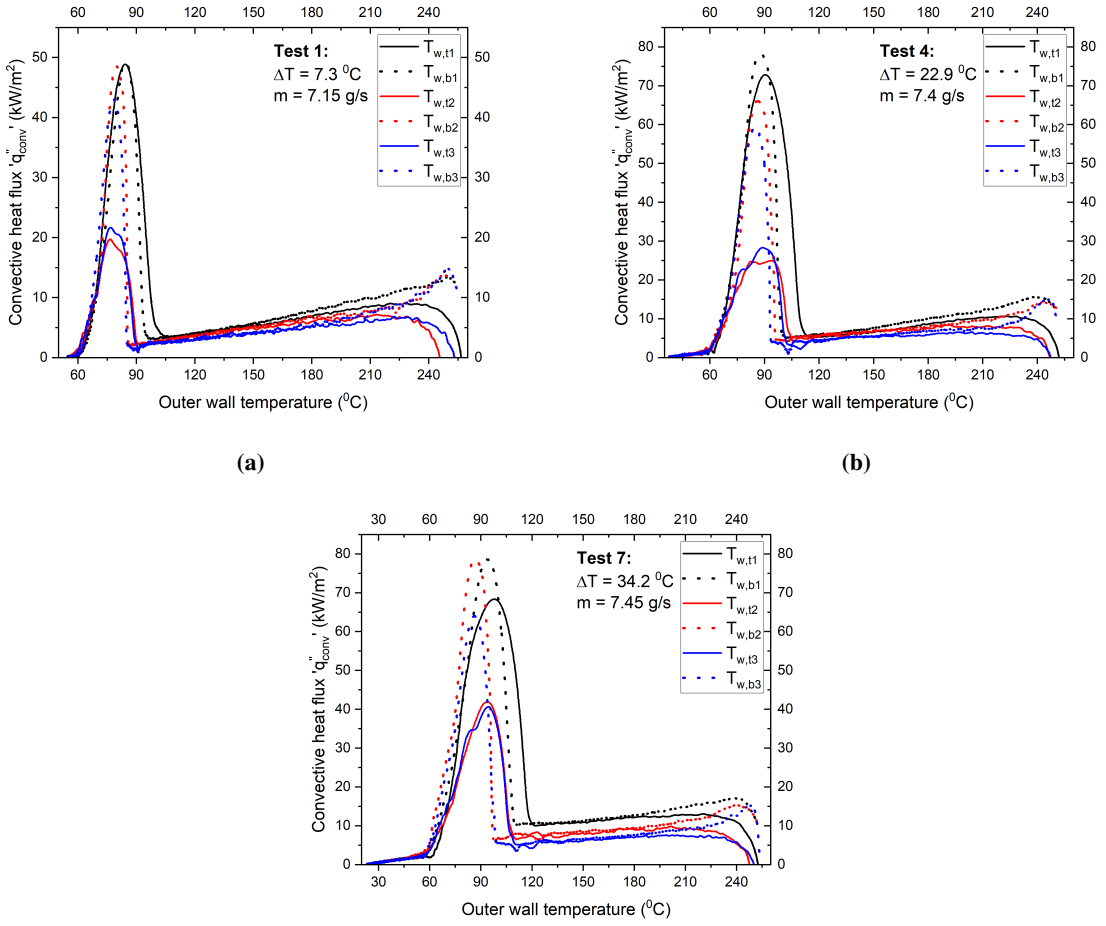

Fig. 5 Convective heat flux curves at different inlet liquid subcooling and wall locations

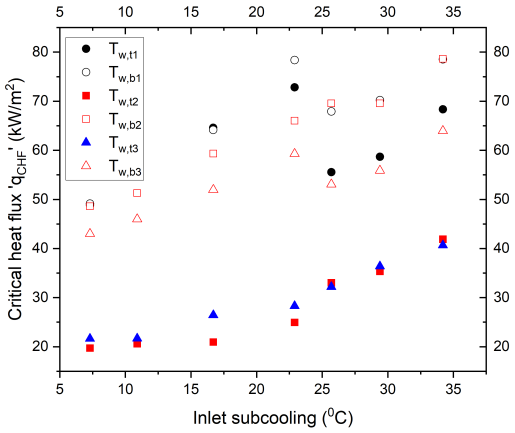

Fig. 6 Effect of inlet liquid subcooling on the critical heat flux values at different wall locations

higher or almost equal to the top wall CHFs due to the effect of gravity in the horizontal chilldown configuration. The upstream wall location 1 show a higher CHF than the downstream wall locations 2 & 3 as the flow inertia reduces in the downstream direction.

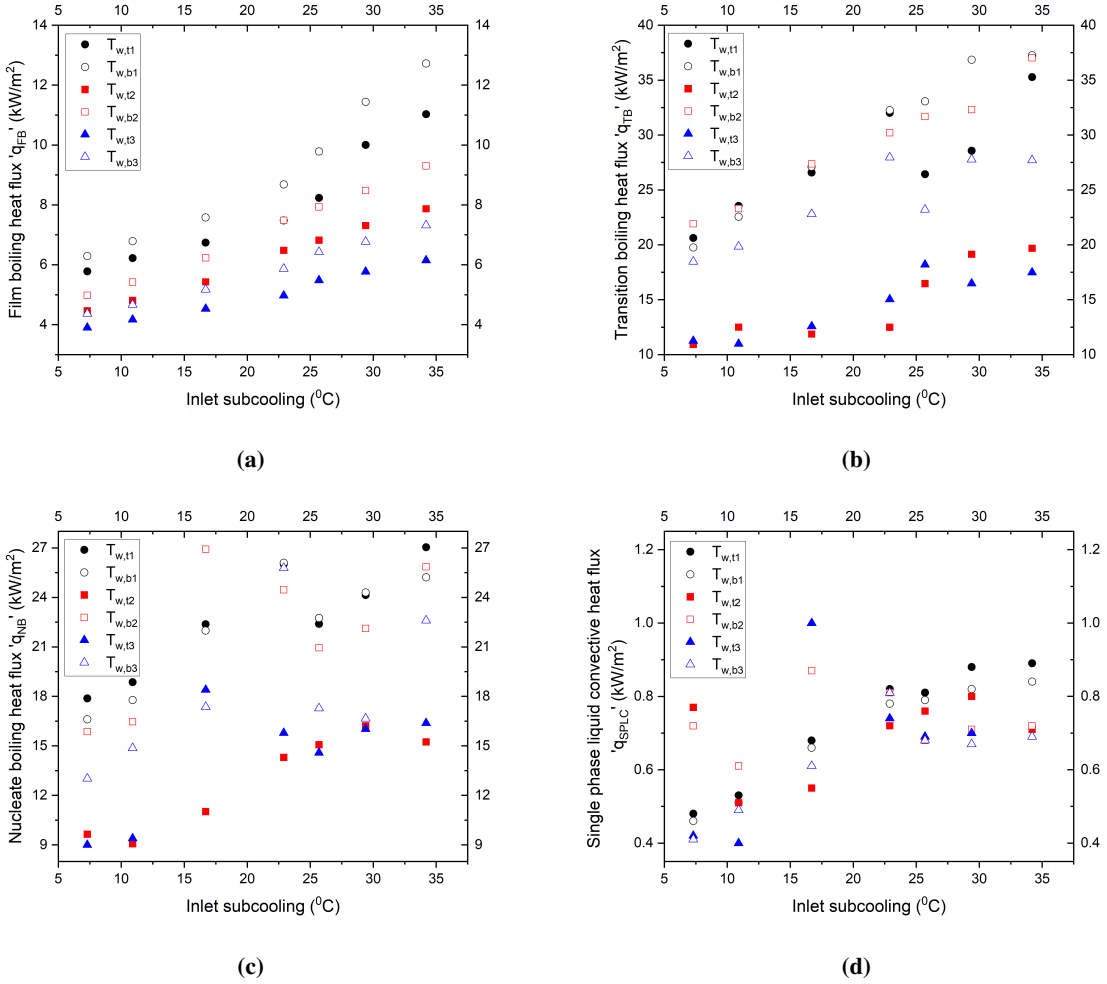

Fig. 7 Effect of inlet liquid subcooling on the time-averaged convective heat flux values for different regimes during the chilldown process at different wall locations

By identifying the chilldown start and end points, rewetting and ONB points, and CHF values, the regime-specific heat fluxes are obtained by time-averaging the heat flux data in different regimes and are plotted at different inlet liquid subcooling and wall locations in Fig. 7. The transition boiling regime shows the highest heat flux values followed by the nucleate boiling, film boiling and single phase liquid convective regimes. In the film boiling regime, the heat fluxes increase with increase in inlet liquid subcooling. The film boiling heat fluxes are higher for bottom wall locations and decrease in the downstream direction. The transition boiling heat fluxes also increase with increase in inlet liquid subcooling and the bottom wall heat flux values are mostly higher or equal to the top wall heat flux values. At the top walls, the transition boiling heat fluxes at upstream wall location 1 are always higher than the downstream wall locations 2 & 3. For the bottom walls, this difference diminishes in the downstream direction.

The nucleate boiling heat fluxes also show a similar trend as the transition boiling heat fluxes where the heat flux values increase with increase in inlet liquid subcooling. Also, the bottom walls show a higher nucleate boiling heat flux than the top wall locations at most of the data points. Though some fluctuations in data are present, in general, the upstream wall location 1 show a higher nucleate boiling heat flux than the downstream wall locations 2 & 3. The single phase liquid convective heat fluxes tend to increase with increase in inlet liquid subcooling though no definitive variations can be inferred for the effect of wall locations.

D. Heat transfer coefficients

In addition to the heat fluxes, the heat transfer coefficients can be calculated for the different regimes during the chilldown process and are plotted as shown in Fig. 8. In general, the nucleate boiling regime showed higher heat transfer coefficients followed by the transition boiling, and film and single phase liquid convective regimes.

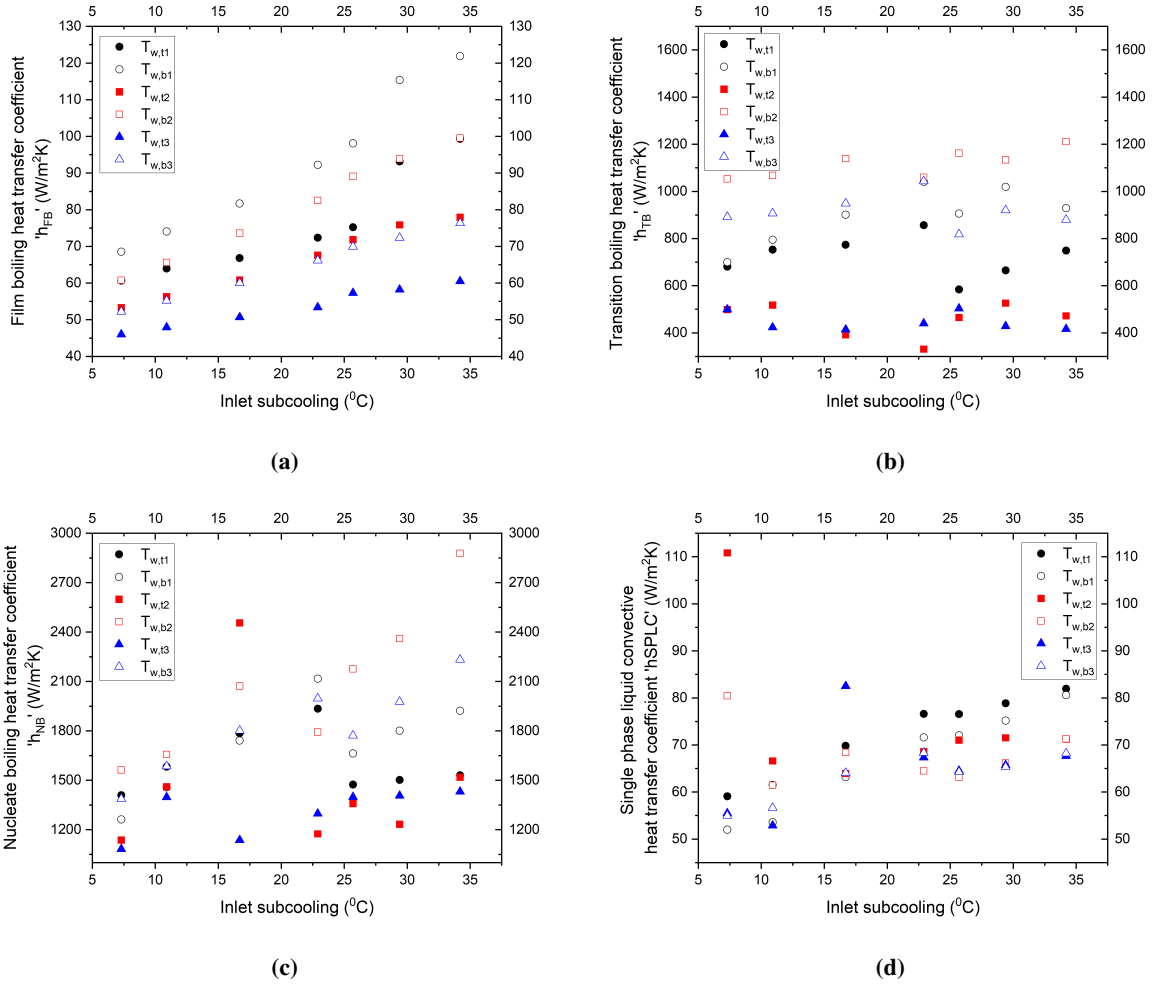

Fig. 8 Effect of inlet liquid subcooling on the time-averaged heat transfer coefficients for different regimes during the chilldown process at different wall locations

Like the film boiling heat fluxes, the film boiling heat transfer coefficients tend to increase with increase in inlet liquid subcooling. The bottom wall film boiling heat transfer coefficients are higher than the top walls and the values tend to decrease in the downstream direction along the test section tube. For the transition boiling regime, no definitive trends were observed for the effect of inlet liquid subcooling whereas the bottom walls showed higher heat transfer coefficients compared to top walls. The nucleate boiling heat transfer coefficients tend to increase with increase in inlet liquid subcooling and the bottom wall heat transfer coefficients are higher than top wall heat transfer coefficients in general. The single phase liquid convection heat transfer coefficients tend to increase with increase in inlet liquid subcooling though no definitive trends were observed for wall locations.

IV. Conclusion

Chilldown experiments were carried out with a simulant fluid PF-5060 through SS-316 tubes to mimic the cryogenic transfer line chilldown process and the entire regimes of the chilldown process were captured in the present study. The effect of inlet liquid subcooling on the chilldown curves, heat flux values and heat transfer coefficients are examined

in detail. In general, the rewetting temperatures, critical heat flux values, regime-specific heat fluxes as well as regime-specific heat transfer coefficients tend to increase with increase in inlet liquid subcooling. Also, the bottom walls exhibit higher rewetting temperatures, heat flux values and heat transfer coefficients than the top walls due to the effect of gravity in the horizontal flow chilldown experiments carried out in the present study. In future, chilldown experiments will be performed at different mass flow rates to verify the effect of inlet liquid subcooling on the chilldown process for a wide range of operating conditions and efforts will be taken to understand the underlying physics.

Acknowledgments

The authors are grateful for the financial support of the National Aeronautics and Space Administration (NASA) under Grant no. 80NSSC22M0056. The authors also acknowledge the machining and fabrication support provided by the Engineering Services Fabrication Center (ESFC) at Case Western Reserve University.

References

[1] Narayanan, J. K., Shingote, C., Huang, C.-N., Pirnstill, L., Kassemi, M., Hartwig, J. W., Mackey, J. R., Pearlman, H. G., and Kharangate, C. R., "Development and Testing of a Two-Phase Flow Chill-down Test Module for Integration with the Flow Boiling and Condensation Experiments at ISS," , 2022. The American Society for Gravitational and Space Research (ASGSR) 2022 Annual Meeting, 9-12 November, Houston, TX, USA.

[2] Darr, S. R., Hu, H., Glikin, N. G., Hartwig, J. W., Majumdar, A., Leclair, A., and Chung, J. N., "An experimental study on terrestrial cryogenic transfer line chilldown I. Effect of mass flux, equilibrium quality, and inlet subcooling," *International Journal of Heat and Mass Transfer*, Vol. 103, 2016, pp. 1225–1242. https://doi.org/10.1016/j.ijheatmasstransfer.2016.05.019.

[3] Darr, S. R., Hu, H., Glikin, N., Hartwig, J. W., Majumdar, A. K., Leclair, A. C., and Chung, J. N., "An experimental study on terrestrial cryogenic tube chilldown II. Effect of flow direction with respect to gravity and new correlation set," *International Journal of Heat and Mass Transfer*, Vol. 103, 2016, pp. 1243–1260. https://doi.org/10.1016/j.ijheatmasstransfer.2016.08.044.

[4] Jin, L., Park, C., Cho, H., Lee, C., and Jeong, S., "Experimental investigation on chill-down process of cryogenic flow line," *Cryogenics*, Vol. 79, 2016, pp. 96–105. https://doi.org/10.1016/j.cryogenics.2016.08.006.

[5] Hartwig, J. W., Styborski, J., McQuillen, J., Rame, E., and Chung, J. N., "Liquid hydrogen line chilldown experiments at high Reynolds Numbers. Optimal chilldown methods," *International Journal of Heat and Mass Transfer*, Vol. 137, 2019, pp. 703–713. https://doi.org/10.1016/j.ijheatmasstransfer.2019.03.090.

[6] Jin, L., Lee, J., and Jeong, S., "Investigation on heat transfer in line chill-down process with various cryogenic fluids," *International Journal of Heat and Mass Transfer*, Vol. 150, 2020, p. 119204. https://doi.org/10.1016/j.ijheatmasstransfer.2019.119204.

[7] Hartwig, J. W., Meyerhofer, P., Stiegemeier, B., and Morehead, R., "Liquid methane and liquid oxygen horizontal chilldown experiments of a 2.54 and 11.43 cm transfer line," *Applied Thermal Engineering*, Vol. 205, 2022, p. 118042. https://doi.org/10.1016/j.applthermaleng.2022.118042.

[8] Jin, L., Cho, H., and Jeong, S., "Experimental investigation on line chill-down process by liquid argon," *Cryogenics*, Vol. 97, 2019, pp. 31–39. https://doi.org/10.1016/j.cryogenics.2018.11.003.

[9] Darr, S. R., Dong, J., Glikin, N., Hartwig, J. W., Majumdar, A., Leclair, A., and Chung, J., "The effect of reduced gravity on cryogenic nitrogen boiling and pipe chilldown," *npj Microgravity*, Vol. 2, 2016. https://doi.org/10.1038/npjmgrav.2016.33.

[10] Hartwig, J. W., Chung, J., Dong, J., Han, B., Wang, H., Darr, S., Taliaferro, M., Jain, S., and Doherty, M., "Nitrogen flow boiling and chilldown experiments in microgravity using pulse flow and low-thermally conductive coatings," *npj Microgravity*, Vol. 8, 2022. https://doi.org/10.1038/s41526-022-00220-9.

[11] Westbye, C. J., Kawaji, M., and Antar, B. N., "Boiling heat transfer in the quenching of a hot tube under microgravity," *Journal of Thermophysics and Heat Transfer*, Vol. 9, No. 2, 1995, pp. 302–307. https://doi.org/10.2514/3.660.

[12] Kawaji, M., Westbye, C. J., and Antar, B. N., "Microgravity experiments on two-phase flow and heat transfer during quenching of a tube and filling of a vessel." *AIChE Symposium Series*, Vol. 87, 1991, pp. 236–243.

[13] Adham-Khodaparast, K., Xu, J., and Kawaji, M., "Flow film boiling collapse and surface rewetting in normal and reduced gravity conditions," *International Journal of Heat and Mass Transfer*, Vol. 38, No. 15, 1995, pp. 2749–2760. https://doi.org/10.1016/0017-9310(95)00026-6.

[14] Celata, G. P., Cumo, M., Gervasi, M., and Zummo, G., "Quenching experiments inside 6.0 mm tube at reduced gravity," *International Journal of Heat and Mass Transfer*, Vol. 52, No. 11, 2009, pp. 2807–2814. https://doi.org/10.1016/j.ijheatmasstransfer.2008.08.043.

[15] Celata, G. P., Cumo, M., D'Annibale, F., Saraceno, L., and Zummo, G., "Rewetting velocity in quenching at reduced gravity," *International Journal of Thermal Sciences*, Vol. 49, No. 9, 2010, pp. 1567–1575. https://doi.org/10.1016/j.ijthermalsci.2010.04.012.

[16] Kharangate, C. R., O'Neill, L. E., Mudawar, I., Hasan, M. M., Nahra, H. K., Balasubramaniam, R., Hall, N. R., Macner, A. M., and Mackey, J. R., "Flow boiling and critical heat flux in horizontal channel with one-sided and double-sided heating," *International Journal of Heat and Mass Transfer*, Vol. 90, 2015, pp. 323–338. https://doi.org/10.1016/j.ijheatmasstransfer.2015.06.073.

[17] Narayanan, J. K., Shingote, C., Qiu, Y., Hartwig, J. W., Mackey, J. R., Kassemi, M., and Kharangate, C. R., "Line Chilldown and Flow Boiling Heat Transfer Characteristics of Stainless Steel Tubes," 2023, p. V001T16A002. https://doi.org/10.1115/HT2023-106318.

[18] Burggraf, O. R., "An Exact Solution of the Inverse Problem in Heat Conduction Theory and Applications," *Journal of Heat Transfer*, Vol. 86, No. 3, 1964, pp. 373–380. https://doi.org/10.1115/1.3688700.